Heliyon 10 (2024) e38344

Contents lists available at ScienceDirect

Heliyon

journal homepage: www.cell.com/heliyon

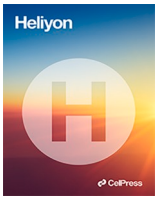

Case report

Case report: Single-cell RNA sequencing of PBMCs highlights monocyte gene expression alterations in a type A HBV-ACLF patient

Yan Wang [a,2], Zengfang Hao [b,2], Jiahua Liu [a,2], Xige Kang [a], Chenguang Ji [a], Yu Guo [a], Zian Chen [a], Jiaao Ma [c], Jin Li [c], Xiaoxu Jin [a], Zhijie Feng [a,**,1], Weicheng Liang [d,***,1], Qi Wei [a,*,1]

[a] *Department of Gastroenterology, The Second Hospital of Hebei Medical University, Hebei Key Laboratory of Gastroenterology, Hebei Institute of Gastroenterology, Hebei Clinical Research Center for Digestive Diseases, Shijiazhuang, China*
[b] *Department of Pathology, The Second Hospital of Hebei Medical University, Shijiazhuang, China*
[c] *Department of Physiology, Hebei Medical University, Shijiazhuang, China*
[d] *Biotherapy Center, The Third Affiliated Hospital of Sun Yat-sen University, Guangzhou, China*

ARTICLE INFO

Keywords:
HBV-Related acute-on-chronic liver failure
Monocytes M1/M2 polarization
Single cell RNA-Seq
Peripheral blood mononuclear cells
Case report

ABSTRACT

Hepatitis B Virus-related acute-on-chronic liver failure (HBV-ACLF) is a severe complication with high fatality rates. However, the underlying mechanisms are still elusive and require further investigation. In this report, we described a case of type A HBV-ACLF in which significant changes were found in monocyte gene expression through single-cell RNA sequencing (scRNA-seq). Furthermore, we observed a shifted M1/M2 polarization as well as dynamic changes in HBV-ACLF markers expression within the circulating monocyte population. The co-expression of HBV-ACLF markers (MERTK, THBS1, PPARγ, and SEMA6B) in the circulating monocyte population suggests that monocytes could play an essential role in the development of HBV-ACLF. By analyzing a public HBV-ACLF cohort with bulk RNA-seq data (64 patients), we showed that the expression level of monocytes marker CD163 gradually increased among normal control individuals (NC, n = 15), patients with liver cirrhosis (LC, n = 10), patients with chronic hepatitis B infection (CHB, n = 10), patients with acute-on-chronic hepatic dysfunction (ACHD, n = 10), and patients with HBV-ACLF (n = 20). Furthermore, the representative HBV-ACLF marker THBS1 was significantly correlated with CD163 in this large clinical cohort. It indicated that the dramatic alteration in monocytes may not be limited to our type A HBV-ACLF patient alone but rather a common phenomenon in HBV-ACLF patients. Collectively, our scRNA-seq analysis showed that the pro-inflammatory status of monocytes had shifted into an anti-inflammatory status in this patient, indicating successful treatment and benign prognosis. Although scRNA-seq is still a time-consuming procedure and difficult to apply in daily clinical practice, this report preliminarily shows the promising potential utility of scRNA-seq in HBV-ACLF patients, by which altered status of monocytes could be unbiasedly detected.

* Corresponding author.
** Corresponding author.
*** Corresponding author.
E-mail addresses: 26300056@hebmu.edu.cn (Z. Feng), liangweicheng11@gmail.com (W. Liang), 28502620@hebmu.edu.cn (Q. Wei).
[1] Contribute equally to this article and should be considered co-corresponding authors.
[2] Contribute equally to this article and should be considered co-first authors.

https://doi.org/10.1016/j.heliyon.2024.e38344
Received 13 July 2023; Received in revised form 22 September 2024; Accepted 23 September 2024
Available online 24 September 2024

1. Introduction

Hepatitis B virus-related acute-on-chronic liver failure (HBV-ACLF) is a severe and potentially fatal complication of chronic hepatitis B virus infection (HBV). HBV-ACLF is distinguished by a sudden worsening of the underlying chronic liver disease, which is often triggered by a precipitating event [1]. Despite its high fatality rates, the underlying mechanisms are still elusive and need further investigation [2]. HBV-ACLF is classified into three subtypes based on the presence or absence of cirrhosis, as well as whether or not the cirrhosis is compensated [3]. Type A HBV-ACLF is characterized by its occurrence in patients without cirrhosis and is associated with better clinical outcomes. Both type B and type C HBV-ACLF patients have cirrhosis. However, type C patients have non-compensated cirrhosis, whereas type B patients have compensated cirrhosis.

HBV-ACLF is characterized by systemic inflammation, which is believed to be associated, at least in part, with the cellular status of circulating immune cells. Previous bulk RNA-seq studies based on circulating immune cells have linked immune-metabolic disorders to HBV-ACLF development [4]. In this report, we described a case of type A HBV-ACLF, in which significant changes were uncovered in monocyte gene expression, through unbiased transcriptomic profiling of circulating immune cells using single-cell RNA sequencing (scRNA-seq). Furthermore, we observed a shifted M1/M2 polarization as well as dynamic changes in HBV-ACLF marker expression within the circulating monocyte population. Our work is the only existing scRNA-seq study on circulating immune cells of HBV-ACLF based on pre-treatment vs post-treatment patterns, providing insight into circulating monocytes changes in type A HBV-ACLF patients.

2. Case report

In March 2021, a 34-year-old male patient with type A HBV-ACLF was admitted to our hospital (Fig. 1A). Despite being diagnosed with HBV 15 years ago, he had not received antiviral therapy. Ten days before being admitted to our hospital, the patient noticed the appearance of jaundice in his skin and sought medical attention at a local hospital. Additionally, liver function tests revealed elevated alanine transaminase (ALT) at 320 U/L, aspartate transaminase (AST) at 323 U/L, total bilirubin (TBIL) at 375.1 μmol/L, direct bilirubin (DBIL) at 272.8 μmol/L, and indirect bilirubin (IBIL) at 102.3 μmol/L. Coagulation tests indicated a prolonged prothrombin time (PT) of 23 seconds, a decreased prothrombin time activity (PTA) to 30.7 %, and an elevated international normalized ratio (INR) to 2.05. The patient was referred to our hospital for further treatment. Upon admission, the patient's serological tests showed positive hepatitis B surface antigen (HBsAg), negative hepatitis B surface antibody (HBsAb), positive hepatitis B e antigen (HBeAg), positive hepatitis B e antibody (HBeAb), and positive hepatitis B core antibody (HBcAb). In the absence of liver cirrhosis and according to the COSSH-ACLF diagnostic criteria, the patient was diagnosed with type A HBV-ACLF. The COSSH-ACLF criteria, established by the Chinese Group on the Study of Severe Hepatitis B (COSSH), offer an alternative approach to diagnosing HBV-ACLF. Unlike the European Association for the Study of the Liver Acute-on-Chronic Liver Failure (EASL-ACLF) criteria, the COSSH-ACLF criteria include patients without cirrhosis. This increased sensitivity enables the identification of approximately 20 % more HBV-ACLF patients, facilitating earlier diagnosis and intervention, which is critical for improving patient outcomes [5]. Following treatment with tenofovir for viral suppression, intravenous piperacillin/tazobactam, and four times of plasma exchanges, the patient exhibited a gradual

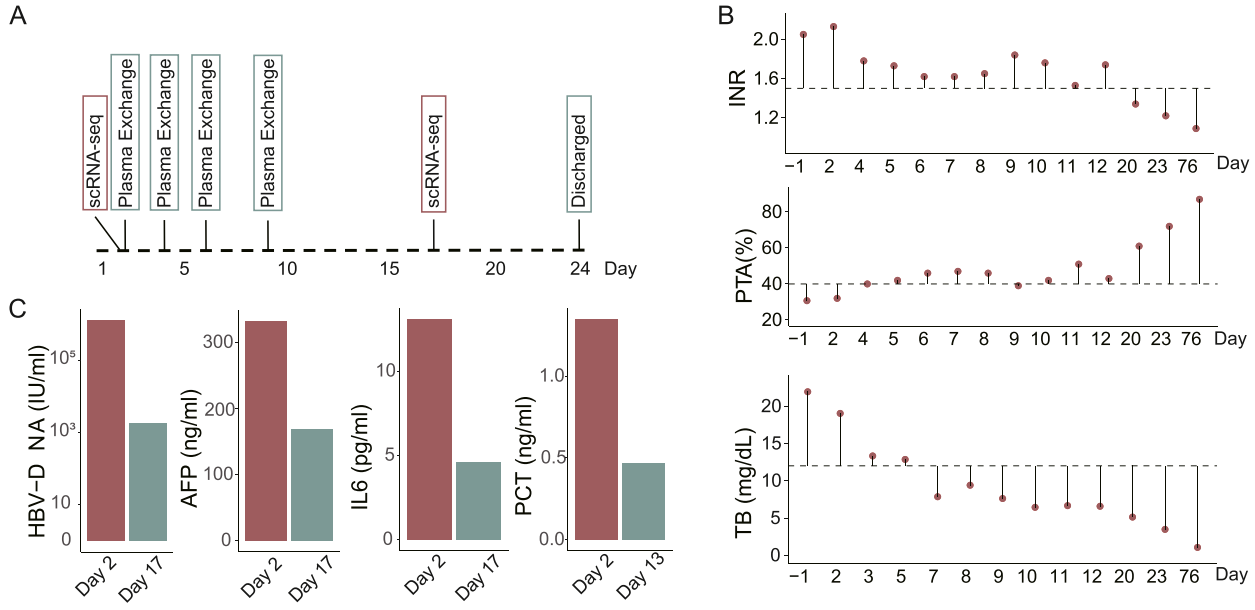

Fig. 1. **(A)** A graphical representation of the clinical timeline. **(B)** Results of laboratory tests for international normalized ratio (INR), prothrombin time activity (PTA), and total bilirubin (TB) during treatment and follow-up. The dashed lines indicated the cut-off value to diagnose HBV-ACLF. **(C)** Results of laboratory tests for HBV-DNA, alpha-fetoprotein (AFP), interleukin 6 (IL6), and procalcitonin (PCT) during treatment.

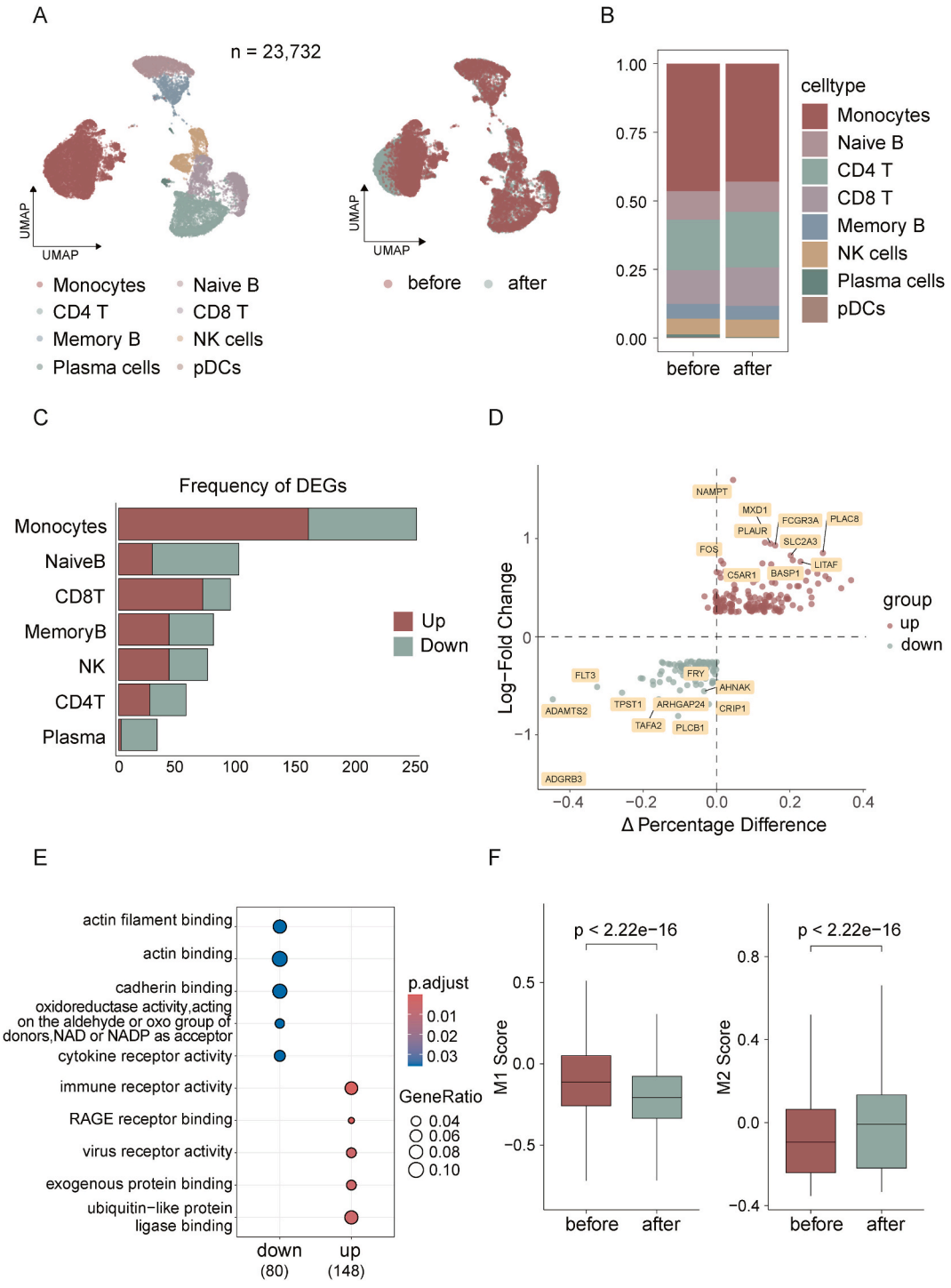

Fig. 2. **(A)** UMAP visualizations depict cell subpopulations (left panel) and contrast the distribution of cell populations before and after treatment (right panel). **(B)** Proportional bar charts illustrate the distribution of cell subpopulations before and after treatment, with each bar color-coded to represent the distinct cell subpopulations identified in this study. **(C)** The bar chart shows the upregulated and downregulated genes in each cell subtype following treatment, identified by |log-fold change| $>$ 0 and an adjusted P value $<$ 0.05 based on the Wilcoxon rank-sum test. **(D)** ΔPercentage difference and log-fold change based on the Wilcoxon rank-sum test results for differential gene expression comparing pre-treatment versus post-treatment in monocytes. Genes highlighted in red or green have |log-fold change| $>$ 0.15 and adjusted p values $<$ 0.05. **(E)** The top 5 GO terms of genes with significant changes in monocytes. Genes in the upregulated group represent biological pathways enriched prior to treatment. **(F)** Comparison of M1 and M2 scores in monocytes between pre-treatment and post-treatment conditions using a *t*-test statistical method. (For interpretation of the references to color in this figure legend, the reader is referred to the Web version of this article.)

resolution of jaundice. Follow-up assessments revealed substantial improvements in liver function, with ALT and AST levels dropping to 42.2 U/L and 34.5 U/L, respectively, and ALB rising to 40.4 g/L. TBIL, DBIL, and IBIL levels decreased significantly to 59.4 μmol/L, 52.10 μmol/L, and 7.30 μmol/L, respectively. Coagulation parameters also improved, as evidenced by a shortened PT to 14s, an increased PA to 72 %, and a decreased INR to 1.22. Inflammation markers such as interleukin-6 (IL6) and procalcitonin (PCT), gradually returned to normal ranges, indicating that treatment was effective (Fig. 1B and C). After being discharged from the hospital, the patient continued the regular oral antiviral therapy. Throughout the follow-up period, the patient did not experience jaundice. Moreover, the INR, PTA, and TB levels of this patient remained within normal ranges.

Single-cell RNA sequencing (scRNA-Seq) is a technique to detect RNA transcripts at the single-cell level in an unprecedented resolution [6], which could contribute to a comprehensive investigation of circulating immune-cell alterations in patients with HBV-ACLF. To investigate immune disorder during the development of HBV-ACLF, we obtained peripheral blood mononuclear cells (PBMCs) from this patient on day 2 and day 17 after the patient signed the informed consent form. These samples were regarded as pre-treated status and post-treated status, respectively. The data of PBMCs samples were subsequently subjected to scRNA-seq and the following bioinformatic analysis (Fig. 2A). When we used the method of uniform manifold approximation and projection (UMAP) to reduce the dimensions of scRNA-seq data, the position of T cells, B cells, NK cells, plasmacytoid dendritic cells and plasma cells overlapped in the post-treated status compared to the pre-treated status. Although the monocyte count exhibited only a mild decrease (Fig. 2B), their altered position in the UMAP projection indicated a significant shift in cellular status following treatment (Fig. 2A). Moreover, monocytes exhibited the highest number of differential expression genes (DEGs) compared to other cell types (Fig. 2C). This indicated a dramatic alteration in the transcriptome of monocytes. To delineate the functional alterations in monocytes associated with treatment, DEGs specific to monocytes were detected. Significant alterations in gene expression for FOS (Fos Proto-Oncogene, AP-1 Transcription Factor Subunit), FLT3 (Fms Related Receptor Tyrosine Kinase 3), and NAMPT (Nicotinamide phosphoribosyltransferase) were observed in monocytes following treatment (Fig. 2D). These genes are pivotal regulators of monocyte function and polarization [7,8]. Enrichment analysis was conducted to reveal the functions of DEGs in pre- and post-treatment (Fig. 2E). Genes highly expressed in pre-treatment status were enriched in functions associated with cellular communication, notably characterized by heightened protein binding and receptor interaction activities. However, in post-treatment status, enrichment shifted towards functions related to increased oxidoreductase activity, cellular architecture proteins such as actin and cadherin, and cytokine binding. Collectively, a shifted cellular status of monocytes in our patient was found based on scRNA-seq analysis.

Monocytes are precursors of macrophages, which can be classified into two categories: pro-inflammatory M1 macrophages and anti-inflammatory M2 macrophages [9]. Monocytes can also be divided into M1 and M2 categories, mirroring the concept of M1/M2 macrophage polarization [10]. By calculating the M1 and M2 scores. We found that, compared with the pre-treated status, the M1 score was decreased while the M2 score was increased in the post-treated status (Fig. 2F). In the pre-treated status, pro-inflammatory monocytes were dominant in the whole monocyte population, while in the post-treated status, anti-inflammatory monocytes were dominant.

Pseudotime analysis was conducted to elucidate the developmental trajectories of monocytes, identifying five distinct monocyte states and delineating a differentiation trajectory from state 1 to state 5 (Fig. 3A). Notably, after treatment, the M1/M2 score ratio significantly decreased across all monocyte states, indicating a shift towards the anti-inflammatory M2 phenotype from the pro-inflammatory M1 phenotype (Fig. 3B). Quantification of monocyte state proportions post-treatment revealed notable increases in states 1 and 2, while states 3, 4, and 5 experienced significant decreases (Fig. 3C). Consequently, treatment to this patient led to an elevated proportion of less differentiated monocytes with a concurrent shift to M2 polarization.

Employing the MacSpectrum tool, we further explored the link between monocyte polarization and differentiation states post-treatment [11]. The tool evaluates inflammation and maturity through the macrophage polarization index (MPI) and the activation-induced macrophage differentiation index (AMDI), respectively, with scores from −50 to 50 reflecting increased severity of inflammation and level of maturity. It revealed a decrease in inflammatory properties across all post-treatment cell states (Fig. 3D). Additionally, a volcano plot identified the top five upregulated and downregulated genes specific to each state (Fig. 3E). In conclusion, treatment to this patient modulates monocyte polarization and differentiation, leading to a transition to states with reduced inflammation and lower differentiation.

Based on recent work by Li et al. [4], it was shown that immune-metabolism disorder is a core axis driving the development of HBV-ACLF. Li and co-workers identified four up-regulated genes (MERTK, THBS1, PPARγ, and SEMA6B) as biomarkers of HBV-ACLF. However, as the study was limited by using bulk RNA-seq of circulating immune cells, the expression profiles of these biomarkers at the single cell levels were largely unknown. Based on our scRNA-seq data, we found that these biomarkers were specifically enriched in the circulating monocyte population (Fig. 4A). Moreover, the RNA levels of these biomarkers were significantly reduced after treatment (Fig. 4B). THBS1 expressed in more than 20 % of monocytes in scRNA-seq data, which may indicate that it could be a more generally expressed marker. The co-expression of HBV-ACLF markers in the circulating monocyte population could not be a coincidence. However, it may be indicated that monocytes could play an essential role in the development of HBV-ACLF.

In order to explore whether there are dramatic alterations of monocytes in other HBV-ACLF patients, we analyzed the gene expression change of monocytes in a large public cohort with bulk RNA-seq data (65 patients) [4]. CD163 is a widely used monocytes-specific marker, and it specifically expressed in the monocyte population in our scRNA-seq data (Fig. 5A). The expression level of CD163 gradually increased among normal control individuals (NC, $n = 15$), patients with liver cirrhosis (LC, $n = 10$), patients with chronic hepatitis B infection (CHB, $n = 10$), patients with acute-on-chronic hepatic dysfunction (ACHD, $n = 10$), and patients with HBV-ACLF ($n = 20$). With the evolving disease course, the monocyte marker CD163 is elevated (Fig. 5B). Furthermore, the representative HBV-ACLF marker THBS1 was significantly correlated with CD163 in this large clinical cohort (Fig. 5C). It indicates that the dramatic alteration in monocytes may be not limited in our type A HBV-ACLF patient alone but rather a very common phenomenon in

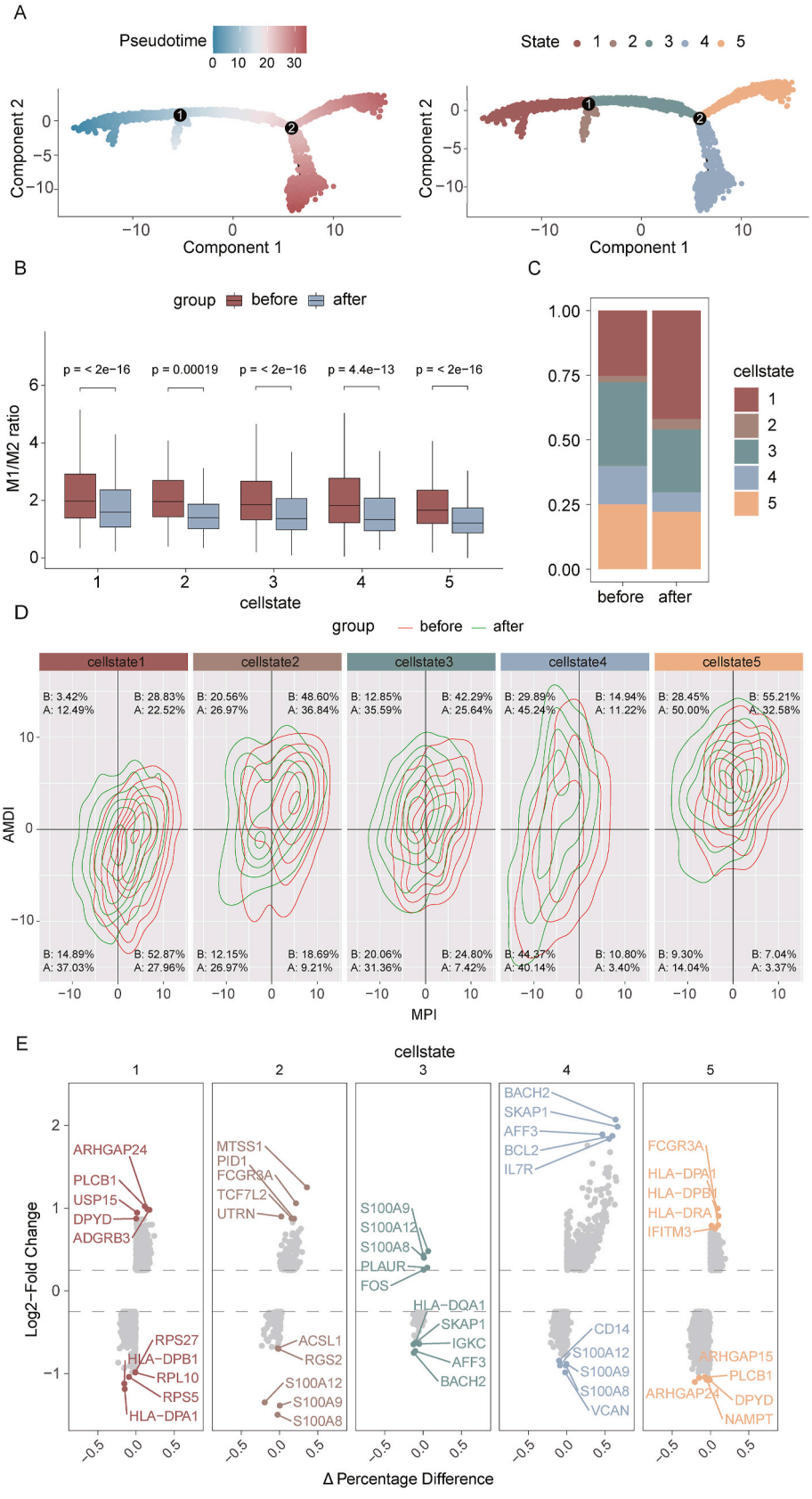

(caption on next page)

Fig. 3. **(A)** Trajectory illustrates the progression of monocyte states from state 1 to state 5, color-coded by pseudotime from cooler to warmer shades for earlier to later stages. **(B)** Comparison of M1/M2 ratio across monocyte states before and after treatment using a *t*-test statistical method. **(C)** The proportion of each monocyte state before and after treatment. **(D)** Radar charts for five different monocyte states before (red lines) and after (green lines) treatment, reflecting changes in the Monocyte Polarization Index (MPI) and the Differentiation Index (AMDI). Percentages denote the proportion of cells within each state before (B) and after (A) treatment. **(E)** Significant differentially expressed genes across the five states of monocytes with a threshold of |log-fold change| > 0.25 and a Wilcoxon test with $p < 0.05$. (For interpretation of the references to color in this figure legend, the reader is referred to the Web version of this article.)

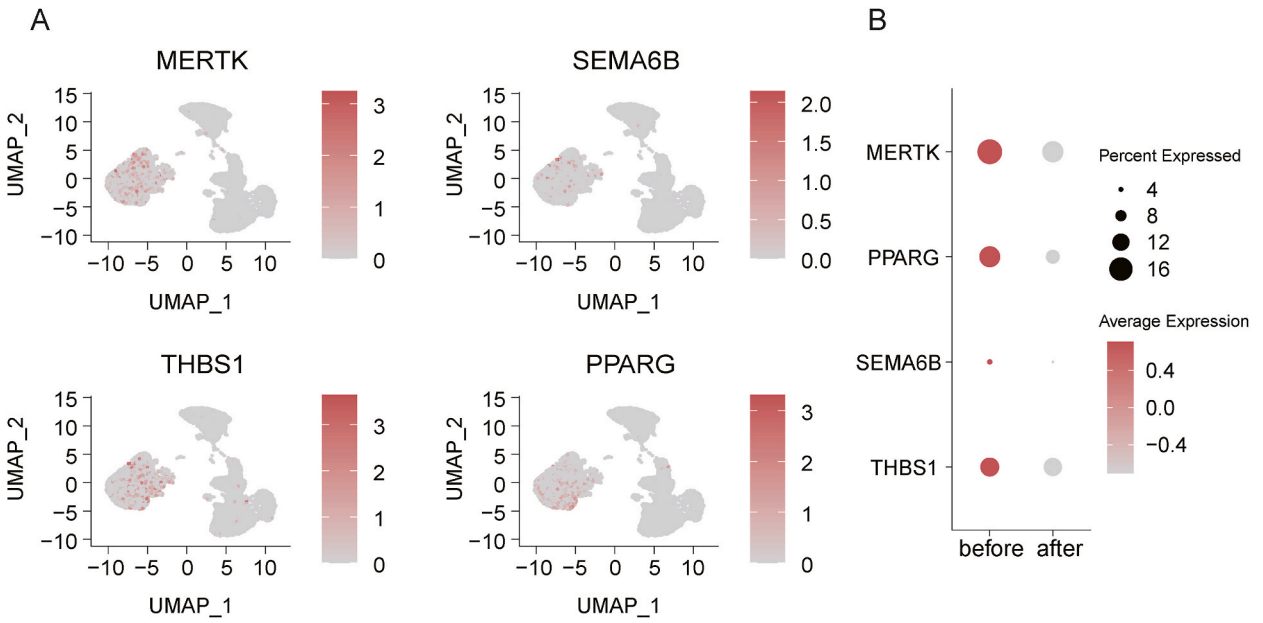

Fig. 4. **(A)** HBV-ACLF markers specifically expressed in monocytes. **(B)** HBV-ACLF markers were up-regulated before treatment compared to after treatment.

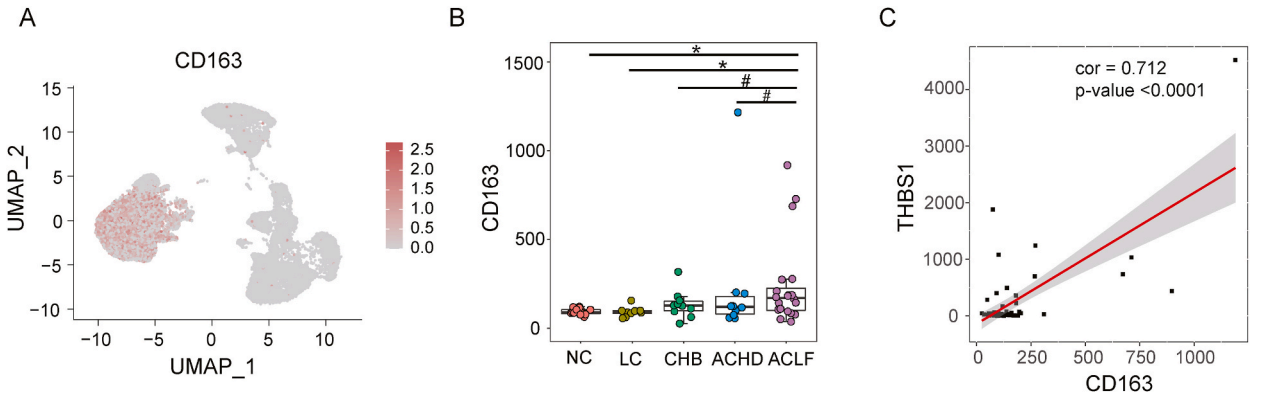

Fig. 5. **(A)** In single-cell RNA-seq data, CD163 is specifically expressed in the monocytes population. **(B)** In bulk RNA-seq data, the expression level of CD163 gradually increased among normal control individuals (NC, n = 15), patients with liver cirrhosis (LC, n = 10), patients with chronic hepatitis B infection (CHB, n = 10), patients with acute-on-chronic hepatic dysfunction (ACHD, n = 10), and patients with HBV-ACLF (n = 20). The statistical significance of CD163 expression difference between each group was evaluated by Wilcoxon rank-sum test. **(C)** In bulk RNA-seq data, the expression of THBS1 correlated with CD163. Spearman's correlation coefficient was used to evaluate the correlation between THBS1 and CD163. * represents with statistical significance. # represents without statistical significance.

other HBV-ACLF patients.

3. Discussion

In this study, we applied scRNA-seq technology to analyze single-cell transcriptomics of PBMCs in a type A HBV-ACLF patient. As we obtained the PBMCs from this patient on day 2 and day 17, it was a self-controlled study. This experimental design effectively removed the batch effect of scRNA-seq caused by individual variation, and could exactly highlight the transcriptional changes in different cell subgroups. Firstly, it was found that transcriptomic status of monocytes dramatically changed, as a larger number of DEGs than other cell types and a significantly shifted position in UMAP analysis. The enrichment analysis further indicated that down-regulated genes post-treatment are associated with inflammation. The decrease in immune receptor activity, including RAGE receptor binding and virus receptor activity, suggests a lower pro-inflammatory response [12]. This shift towards an anti-inflammatory state likely contributes to the mitigation of inflammatory processes, promoting a more balanced immune response and aiding in recovery. Secondly, it was indicated that M1/M2 monocytes polarization in pre-treatment status was imbalanced. Pro-inflammatory monocytes were dominant in whole monocyte population in the pre-treated status, whereas in the post-treated status, anti-inflammatory monocytes were dominant. Utilizing Monocle2, our study identified five discrete monocyte states and observed a notable decrease in the M1/M2 ratio following treatment, indicating a polarization shift towards the M2 phenotype (Fig. 3). The treatment induced an increased proportion of less differentiated cells and a concurrent decline in the count of more differentiated cells, implying a selective expansion of immature monocytes. Further validated by MacSpectrum, the treatment's effect on reducing monocyte inflammation was confirmed across all differentiation states. Thirdly, previously reported four HBV-ACLF markers (MERTK, THBS1, PPARγ, and SEMA6B) were uncovered highly enriched in the circulating monocyte population, and their expression is significantly increased in the pre-treatment stage of this patient. Although this is just a case report and only one patient was included in our study, we intriguingly found that monocytes may play an essential function during the development of type A HBV-ACLF. Moreover, by analyzing a public HBV-ACLF cohort with bulk RNA-seq data (64 patients), we showed that THBS1 was significantly correlated with the widely-accepted monocyte marker CD163. Moreover, the expression level of CD163 gradually increased among normal control individuals, patients with liver cirrhosis, patients with chronic hepatitis B infection, patients with acute-on-chronic hepatic dysfunction, and patients with HBV-ACLF. It may be indicated that the dramatic alteration in monocytes may be not limited in our type A HBV-ACLF patient alone.

Monocytes/macrophages are a cell population highly enriched in liver tissue, and are critical for maintaining the capability of rapid responses to hepatic injury [9]. Kupffer cells are those liver macrophages derived from the local progenitors, maintaining the self-renewal capability during normal homeostasis. In the presence of hepatic injury, infiltrating bone-marrow derived monocytes could rapidly compensate the exhausted pool of Kupffer cells [13]. It is also held true for HBV-ACLF patients. Previous study by Zhang et al. [14] based on scRNA-seq has revealed that abundant monocyte/macrophages infiltrated into the liver tissue of HBV-ACLF patients. However, Zhang and co-workers only investigated liver tissue and did not analyze the transcriptome of PBMCs, which is the origin of monocyte-derived macrophages. Similar to our work, recent study by Jia et al. investigated circulating monocytes of HBV-ACLF patients based on scRNA-seq [15], including 6 HBV-ACLF patients and 3 healthy controls. But, our work is still the only existed scRNA-seq study on circulating immune cells of HBV-ACLF based on pre-treatment *vs* post-treatment patterns. However, the ideal approach would be to study circulating immune cells and liver tissue of HBV-ACLF simultaneously, as in this case, the process of infiltrating bone-marrow derived monocytes in liver tissue could be illustrated. In the research of cirrhosis by Ramachandran et al. [16], pseudotemporal trajectory from circulating monocytes to cirrhosis-related macrophages had been illustrated by *in silico* trajectory analysis on a combined dataset including both PBMC and immune cells resided in liver tissue. Currently, the pseudotemporal trajectory from circulating monocytes to ACLF-related macrophages has not been illustrated.

There are still knowledge gaps in the study of circulating monocytes of HBV-ACLF. Different subtypes of HBV-ACLF may exhibit distinct alterations. This case was a younger patient with type A HBV-ACLF and was assumed to be without immunosenescence. Although the monocyte markers alteration was validated by a large cohort, it was still unknown whether the robustly shifted monocyte polarization exists in type B and type C HBV-ACLF patients. Type B and type C HBV-ACLF patients are typically older and have cirrhosis with or without compensation, which may be with the occurrence of immunosenescence or exhausted immune system. Previous studies by Zhang et al. [14] and Jia et al. [15] had limited sample sizes and no distinct classification for the subtypes of patients. Establishing a larger cohort that can identify immune discrepancies among each subtype of HBV-ACLF is an aim that needs to be realized in the future.

Moreover, our study failed to distinguish which treatment is the most essential one leading to the transcriptomics alterations in single cell level. In addition to plasma exchange and oral antiviral therapy with tenofovir, the patient also received intravenous piperacillin/tazobactam. Our current case report focuses on the integrated effects of the treatment as a whole, and the genes alteration observed in scRNA-seq analysis resulting from the treatment's synergistic effects. The specific contributions of each treatment still need further investigation.

4. Conclusion

In this report, we described a case of type A HBV-ACLF, in which robustly shifted polarization was observed in monocytes by scRNA-seq analysis. Moreover, dynamic changes in HBV-ACLF markers expression within the circulating monocyte population were detected and subsequently validated by a big clinical cohort with bulk RNA-seq data. Although scRNA-seq is still a time-consuming procedure that may be difficult to apply in daily clinical practice, this report preliminarily shows the potential promising utility of scRNA-seq in HBV-ACLF patients, by which altered status of monocytes can be unbiasedly detected. In the future, next-generation

technology derived from scRNA-seq may be applicable in clinical decision-making for diagnosis and treatment, not only for HBV-ACLF but also for various other clinical applications [17].

Ethics statement

This study was reviewed and approved by the Research Ethics Committee of the Second Hospital of Hebei Medical University, with the approval number 2020-C033, dated June 1, 2020.

The patient provided written informed consent to participate in the study and for his data to be published. Informed consent was obtained in accordance with the guidelines and approval from the Research Ethics Committee of the Second Hospital of Hebei Medical University.

Data availability

The raw sequence data reported in this paper have been deposited in the Genome Sequence Archive in National Genomics Data Center, China National Center for Bioinformation/Beijing Institute of Genomics, Chinese Academy of Sciences (GSA-Human: HRA007641) that are publicly accessible at https://ngdc.cncb.ac.cn/gsa-human ([18,19])

Funding

This work was supported by grants from >Basic and Applied Basic Research Scheme (2023B03J1348 and 2023A03J0197 to WL, S&T Program of Hebei (22377705D to YW), the National Natural Science Foundation of China (81700547 to YW), Key Science and Technology Research Program of Health Commission of Hebei Province (20210531 to YW), Hebei Natural Science Foundation (H2021206314 to WQ), and S&T Program of Hebei (22377703D to ZF).

CRediT authorship contribution statement

Yan Wang: Writing – original draft, Validation, Project administration, Methodology, Investigation, Funding acquisition, Formal analysis, Data curation, Conceptualization. **Zengfang Hao:** Software, Resources, Methodology, Investigation, Formal analysis. **Jiahua Liu:** Writing – review & editing, Visualization, Software, Methodology, Investigation, Formal analysis, Data curation. **Xige Kang:** Investigation. **Chenguang Ji:** Resources. **Yu Guo:** Resources, Funding acquisition. **Zian Chen:** Software, Resources. **Jiaao Ma:** Methodology, Investigation. **Jin Li:** Investigation. **Xiaoxu Jin:** Methodology, Investigation. **Zhijie Feng:** Writing – review & editing, Validation, Supervision, Resources, Funding acquisition. **Weicheng Liang:** Writing – review & editing, Writing – original draft, Visualization, Validation, Supervision, Conceptualization. **Qi Wei:** Writing – review & editing, Writing – original draft, Visualization, Validation, Supervision, Project administration, Methodology, Investigation, Funding acquisition, Conceptualization.

Declaration of competing interest

The authors declare that they have no known competing financial interests or personal relationships that could have appeared to influence the work reported in this paper.

Methods

Patients recruitment

The study protocol was approved by the Research Ethics Committee of the Second Hospital of Hebei Medical University (2020-C033). A patient diagnosed as ACLF by COSSH-ACLF criteria was recruited to our study, and circulating immune cells (peripheral blood mononuclear cells, PBMCs) was isolated and subjected to scRNA-seq. The patient were well informed, and written consent was obtained.

COSSH-ACLF diagnosis criteria

Regardless of the presence of cirrhosis, patients with chronic hepatitis B, TB $\geq$ 12 mg/dL and INR $\geq$1.5 should be diagnosed with ACLF [5].

Single-cell RNA-seq

Cell Capture was performed byusing single cell 3 'Library and Gel Bead Kit V3.1 (10x Genomics, 1000075) and Chromium Single Cell B Chip Kit (10x Genomics, 1000074). After the cDNA was generated and then amplified, and quality assessed using an Agilent 4200. According to the manufacture's introduction, single-cell RNA-seq libraries were constructed using Single Cell 3′ Library and Gel Bead Kit V3.1. The libraries were finally sequenced using an Illumina Novaseq 6000 sequencer.(performed by CapitalBio Technology, Beijing). Feature-barcode matrix was generated by the analysis based on Cellranger. The standard processing workflow for the scRNA-

seq data, encompassing quality control, data normalization, and scaling, was executed by the Seurat R package (V4.4.0) [20]. Poor-quality cells with unique feature counts <800 or >6000, and >10 % mitochondrial counts were filtered, leaving 12932 pre-treatment and 10800 post-treatment cells for further analytical processing. The data removing unqualified cells was further normalized by the global-scaling normalization method "LogNormalize". Utilizing the FindVariableFeatures function, we identified genes exhibiting high variability, with the default setting returning 2000 features. By a linear transformation facilitated by ScaleData, principal component analysis (PCA)was employed to achieve linear dimensional reduction. The top 20 principal components were harnessed for projection in the UMAP visualization and clustering. Cell clustering was accomplished using the FindClusters function, set at a resolution of 0.5.

M1 and M2 score analysis

The M1 and M2 score of monocytes was calulated by the function of AddModuleScore in the packge of Seurat. The M1 score was generated by the expression of CD68, CD80, CD86, FCGR1A, CLEC7A, FCGR2A, FCGR3A. The M2 score was generated by the expression of CSF1R, CD163, MRC1, CD209.

The analysis of differential expression genes (DEGs)

The FindMarkers function with the default parameters (adjusted P-value <0.05 in Wilcoxon rank-sum test, |Log2 FC| > 0.15) wasused to identify differentially expressed genes between pre-treatment and post-treatment in monocytes.

Gene Ontology (GO) pathway analysis

Gene Ontology (GO) biological process (http://geneontology.org/) analysis was performed to investigate monocytes, identifying the top 5 GO terms based on p-value ranking. The threshold for enrichment significance was set at an adjusted p-value of less than 0.05.

Pseudo-time analysis

Monocle 2 with the DDRTree method and default parameters was utilized to analyze single-cell trajectories [21,22]. Firstly, a cell data set object was created for the proposed pseudotime analysis using the newCellDataSet function. Subsequently, the highly variable genes were identified by employing the detectGenes function. Finally, the cell differentiation trajectories were inferred based on the highly variable genes.

MacSpectrum online analysis

The MacSpectrum tool [11] was utilized to evaluate monocyte characteristics by calculating two indices: the Macrophage Polarization Index (MPI) and the Activation-Induced Macrophage Differentiation Index (AMDI). The MPI reflects the inflammatory status of monocytes, while the AMDI indicates the maturity of macrophages. The indices were calculated based on the expression of specific marker genes associated with monocyte polarization and differentiation. The distribution of MPI and AMDI scores was visualized using density plots to demonstrate the treatment's effect on monocyte polarization and differentiation. The online analysis tool for MacSpectrum is available at https://macspectrum.uconn.edu/.

The analysis of CD163 expression in PRJNA548207

The fastq files of PRJNA548207 (https://www.ncbi.nlm.nih.gov/bioproject/PRJNA548207/) was downloaded. The software of Trim Galore was used for adapter trimming. Alignment was performed by STAR, and the BAM files was subjected to counting reads by featureCounts. Subsquently, gene counts was converted to transcripts per million (TPM). The statistical significance of CD163 expression difference were evaluated by Wilcoxon rank-sum test. The expression of CD163 and its correlation with the mean expression of THBS1 was illustrated by ggplot2, and Spearman's correlation coefficient was used to evaluate the correlation between the variables.

References

[1] Q. Li, J. Wang, M. Lu, Y. Qiu, H. Lu, Acute-on-Chronic liver failure from chronic-hepatitis-B, Who is the behind scenes, Front. Microbiol. 11 (2020) 583423.
[2] W. Bernal, R. Jalan, A. Quaglia, K. Simpson, J. Wendon, A. Burroughs, Acute-on-chronic liver failure, Lancet 386 (10003) (2015) 1576–1587.
[3] X. Liu, J. Zhang, X. Wei, Z. Duan, H. Liu, Y. Chen, et al., HBV-related acute-on-chronic liver failure with underlying chronic hepatitis has superior survival compared to cirrhosis, Eur. J. Gastroenterol. Hepatol. 33 (1S Suppl 1) (2021) e734–e739.
[4] J. Li, X. Liang, J. Jiang, L. Yang, J. Xin, D. Shi, et al., PBMC transcriptomics identifies immune-metabolism disorder during the development of HBV-ACLF, Gut 71 (1) (2022) 163–175.
[5] T. Wu, J. Li, L. Shao, J. Xin, L. Jiang, Q. Zhou, et al., Development of diagnostic criteria and a prognostic score for hepatitis B virus-related acute-on-chronic liver failure, Gut 67 (12) (2018) 2181–2191.

[6] W. Liang, Z. Feng, S. Rao, C. Xiao, X. Xue, Z. Lin, et al., Diarrhoea may be underestimated: a missing link in 2019 novel coronavirus, Gut 69 (6) (2020) 1141–1143.
[7] P.J. Sung, M. Selvam, S.S. Riedel, H.M. Xie, K. Bryant, B. Manning, et al., FLT3 tyrosine kinase inhibition modulates PRC2 and promotes differentiation in acute myeloid leukemia, Leukemia 38 (2) (2024 Jan 5) 291–301.
[8] H. Yuan, P. Zhang, Y. Xin, Z. Liu, B. Gao, Single cell RNA-seq identifies a FOS/JUN-related monocyte signature associated with clinical response of heart failure patients with mesenchymal stem cell therapy, Aging (Albany NY) 16 (6) (2024 Mar 20) 5651–5675.
[9] L. Bai, M. Kong, Z. Duan, S. Liu, S. Zheng, Y. Chen, M2-like macrophages exert hepatoprotection in acute-on-chronic liver failure through inhibiting necroptosis-S100A9-necroinflammation axis, Cell Death Dis. 12 (1) (2021) 93.
[10] S. Fukui, N. Iwamoto, A. Takatani, T. Igawa, T. Shimizu, M. Umeda, et al., M1 and M2 monocytes in rheumatoid arthritis: a contribution of imbalance of M1/M2 monocytes to osteoclastogenesis, Front. Immunol. 8 (2017) 1958.
[11] C. Li, A. Menoret, C. Farragher, Z. Ouyang, C. Bonin, P. Holvoet, et al., Single cell transcriptomics based-MacSpectrum reveals novel macrophage activation signatures in diseases, JCI Insight 5 (10) (2019 Apr 16) e126453.
[12] H. Dong, Y. Zhang, Y. Huang, H. Deng, Pathophysiology of RAGE in inflammatory diseases, Front. Immunol. 13 (2022 Jul 29).
[13] E. Gomez Perdiguero, K. Klapproth, C. Schulz, K. Busch, E. Azzoni, L. Crozet, et al., Tissue-resident macrophages originate from yolk-sac-derived erythro-myeloid progenitors, Nature 518 (7540) (2015) 547–551.
[14] P. Zhang, H. Li, C. Zhou, K. Liu, B. Peng, X. She, et al., Single-cell RNA transcriptomics reveals the state of hepatic lymphatic endothelial cells in hepatitis B virus-related acute-on-chronic liver failure, J. Clin. Med. 11 (10) (2022).
[15] J. Yao, T. Liu, Q. Zhao, Y. Ji, J. Bai, H. Wang, et al., Genetic landscape and immune mechanism of monocytes associated with the progression of acute-on-chronic liver failure, Hepatol Int 17 (3) (2023) 676–688.
[16] P. Ramachandran, R. Dobie, J.R. Wilson-Kanamori, E.F. Dora, B.E.P. Henderson, N.T. Luu, et al., Resolving the fibrotic niche of human liver cirrhosis at single-cell level, Nature 575 (7783) (2019) 512–518.
[17] X. Liu, C.A. Powell, X. Wang, Forward single-cell sequencing into clinical application: understanding of cancer microenvironment at single-cell solution, Clin. Transl. Med. 12 (4) (2022) e782.
[18] T. Chen, X. Chen, S. Zhang, J. Zhu, B. Tang, A. Wang, et al., The Genome sequence archive family: toward explosive data growth and diverse data types, Dev. Reprod. Biol. 19 (4) (2021 Aug 1) 578–583.
[19] CNCB-NGDC Members, Xue Y. Partners, Y. Bao, Z. Zhang, W. Zhao, J. Xiao, et al., Database Resources of the national Genomics data center, China national center for bioinformation in 2022, Nucleic Acids Res. 50 (D1) (2021 Oct 28) D27–D38.
[20] Y. Hao, S. Hao, E. Andersen-Nissen, W.M. Mauck, S. Zheng, A. Butler, et al., Integrated analysis of multimodal single-cell data, Cell 184 (13) (2021 Jun) 3573–3587.e29.
[21] X. Qiu, A. Hill, J. Packer, D. Lin, Y.A. Ma, C. Trapnell, Single-cell mRNA quantification and differential analysis with Census, Nat. Methods 14 (3) (2017 Mar) 309–315.
[22] X. Qiu, Q. Mao, Y. Tang, L. Wang, R. Chawla, H.A. Pliner, et al., Reversed graph embedding resolves complex single-cell trajectories, Nat. Methods 14 (10) (2017 Aug 21) 979–982.